



Quark Matter 2015

Measurements of heavy-flavour production in p–Pb collisions with ALICE

Jeremy Wilkinson, for the ALICE Collaboration

Physikalisches Institut, Ruprecht-Karls-Universität Heidelberg, Germany

Abstract

The production of open heavy-flavour particles was studied in p–Pb collisions at $\sqrt{s_{NN}} = 5.02$ TeV using the ALICE detector. Three separate observables were used: the hadronic decays of D mesons at mid-rapidity, and semileptonic decays of heavy-flavour hadrons to electrons and muons at mid-rapidity and forward rapidity, respectively. The most recent ALICE measurements of the nuclear modification factor, R_{pPb} , of open charm and beauty are reported, along with the centrality and multiplicity dependence of D-meson production in p–Pb collisions.

Keywords: Heavy flavour, Nuclear modification factor, pA collisions

1. Introduction

Measurements of heavy-quark (charm and beauty) production offer a unique probe of the properties of the Quark-Gluon Plasma (QGP) produced in ultrarelativistic heavy-ion collisions. Due to their large masses, charm and beauty quarks are predominantly produced in the initial hard scatterings of a heavy-ion collision, rather than in thermal processes at later times, meaning that they experience the full evolution of the collision system, and also that their production is described well by calculations of perturbative Quantum Chromodynamics (pQCD). Measurements of open heavy-flavour production in p–Pb collisions make it possible to disentangle Cold Nuclear Matter (CNM) effects, such as transverse momentum broadening and the modification of nuclear parton distribution functions, from final-state effects that occur in the Quark-Gluon Plasma (QGP) formed in Pb–Pb collisions.

A brief overview of the detectors and analysis strategies used for heavy-flavour measurements is given in the following paragraphs; full details of the ALICE detector and its performance can be found in [1].

Prompt D mesons [2] are reconstructed via the hadronic decay channels $D^0 \rightarrow K^- \pi^+$, $D^+ \rightarrow K^- \pi^+ \pi^+$, $D^{*+} \rightarrow D^0 \pi^+ \rightarrow K^- \pi^+ \pi^+$, and $D_s^+ \rightarrow \phi \pi^+ \rightarrow K^- K^+ \pi^+$. The Inner Tracking System (ITS) comprises six layers of silicon pixel, drift, and strip detectors, and is used for the tracking of charged particles and the reconstruction of the primary and secondary vertices. Track reconstruction in the central barrel ($|\eta| < 0.9$) starts from the large Time Projection Chamber (TPC), which also provides particle identification (PID) by

Email address: jeremy.wilkinson@cern.ch (Jeremy Wilkinson)

measuring the specific energy loss dE/dx of charged particles passing through it. Further PID information is given by the Time Of Flight detector (TOF) via the flight times of charged particles. The V0 scintillator array is used for the minimum-bias trigger. The Silicon Pixel Detector (SPD), the V0A detector, and the Zero-Degree Neutron Calorimeter (ZNA) are used to classify the charged-particle multiplicity and centrality of p–Pb collisions. D-meson candidates are selected based on PID of the decay tracks and the D-meson decay topology, for example by selecting on the impact parameters of the decay tracks and the pointing angle between the reconstructed D-meson momentum and its flight line.

The analysis of electrons from heavy-flavour hadron decays [3] also uses the ITS, TPC and TOF. The Transition Radiation Detector (TRD) and the Electromagnetic Calorimeter (EMCal) provide further triggering and PID at intermediate to high p_T . Background electrons from known hadronic decays are statistically subtracted from the inclusive electron yields, while photon conversions and Dalitz decays are removed via an invariant mass method.

Muons from heavy-flavour hadron decays [4] are identified at forward and backward rapidity¹ using the muon spectrometer. This detector covers $-4.0 < \eta < -2.5$ and consists of a front absorber, a series of tracking chambers, a large dipole magnet, and a set of triggering chambers that sit behind a filter wall. As well as providing an effective trigger for muons, the trigger chambers also allow the rejection of background from punch-through hadrons. Muons from π and K decays are subtracted via data-tuned Monte Carlo simulations.

2. Results

The nuclear modification factor, R_{pPb} , is calculated as $R_{pPb} = \frac{d\sigma_{pPb}/dp_T}{A \cdot d\sigma_{pp}/dp_T}$, where A is the mass number of the Pb nucleus, and σ_{pPb} and σ_{pp} are, respectively, the particle production cross section in p–Pb collisions at $\sqrt{s_{NN}} = 5.02$ TeV and in pp collisions. Reference data were taken for pp collisions at $\sqrt{s} = 2.76$ TeV and $\sqrt{s} = 7$ TeV, and scaled to $\sqrt{s} = 5.02$ TeV using FONLL calculations [5].

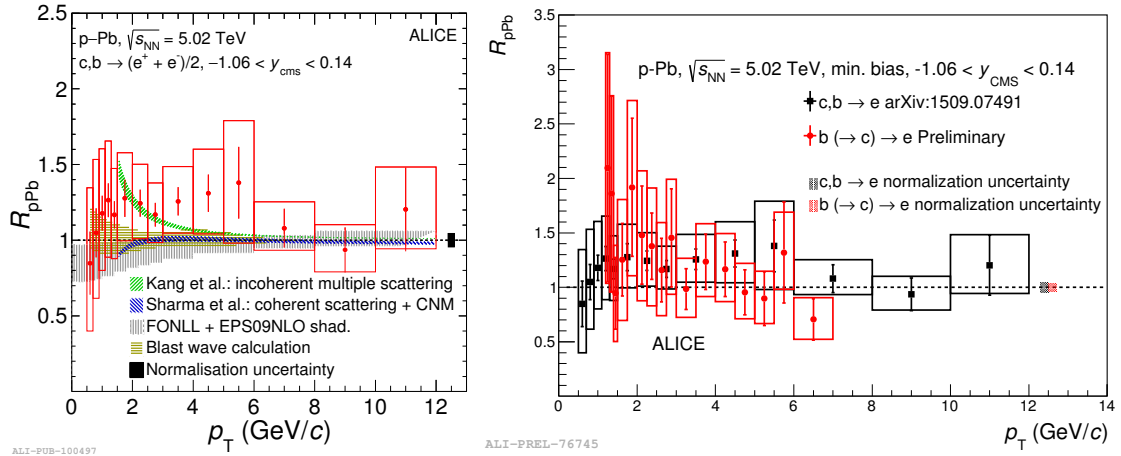


Fig. 1. Left: R_{pPb} of inclusive electrons from heavy-flavour hadron decays [3], compared with models [5–9]. Right: Preliminary beauty-hadron decay electron R_{pPb} (red) compared with the overall R_{pPb} of electrons from heavy-flavour hadron decays (black).

Figure 1 (left) shows the R_{pPb} of electrons from heavy-flavour hadron decays (i.e. those originating from both charm and beauty) [3]. The results are consistent with unity within uncertainties, implying that CNM effects have a negligible effect on heavy-flavour production at high p_T . The R_{pPb} is also reproduced by a variety of model calculations [5–9]. It is also possible to separate the contributions of charm and beauty

¹Per ALICE convention, in p–Pb collisions, the Pb-going direction is referred to as ‘backward’ (negative) rapidity, and the p-going direction is referred to as ‘forward’ (positive) rapidity.

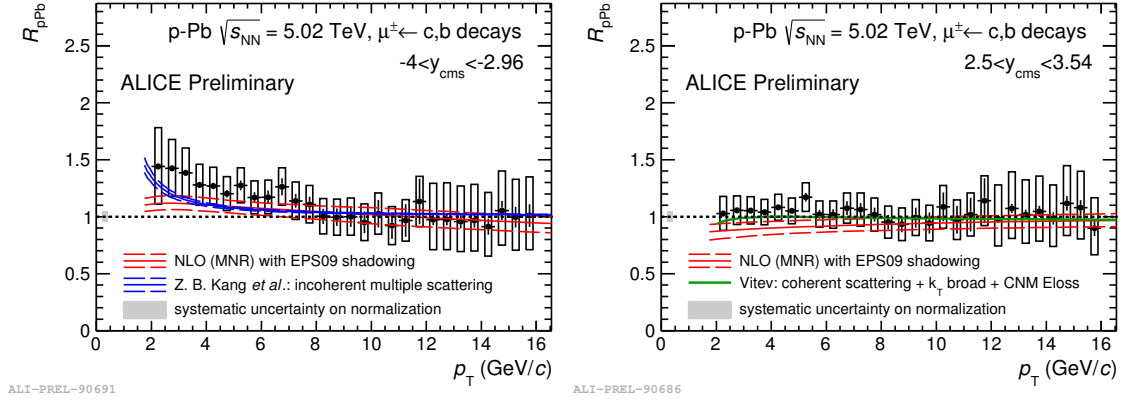


Fig. 2. R_{pPb} of muons from heavy-flavour hadron decays in two rapidity regions, compared with models [8–11]. Left: backward rapidity ($-4 < y_{cms} < -2.96$). Right: forward rapidity ($2.5 < y_{cms} < 3.54$).

production via the impact parameter distributions of the decay products, as it is expected that this distribution will be broader for beauty than charm due to a larger separation between the primary and secondary vertices. The R_{pPb} of inclusive heavy-flavour and beauty-decay electrons are compared in Fig. 1 (right); both results are consistent with unity and with one another within the uncertainties.

The left (right) panel of Fig. 2 shows the R_{pPb} results for muons from heavy-flavour hadron decays at backward (forward) rapidity. The R_{pPb} results at forward rapidity are consistent with unity at all p_T , as was observed for electrons from heavy-flavour hadron decays at mid-rapidity. At backward rapidity, the R_{pPb} is also consistent with unity for $p_T > 4$ GeV/c, however there is an enhancement above unity for $2 < p_T < 4$ GeV/c. The results in both rapidity regions are replicated within uncertainties by models [8–11].

Figure 3 (left) shows the average R_{pPb} of prompt D^0 , D^+ and D^{*+} mesons as a function of p_T [2]. The R_{pPb} of D mesons is consistent with unity for $p_T > 2$ GeV/c, and is described by calculations that include CNM effects [7, 9, 11–13]. By contrast, the nuclear modification factor in Pb–Pb collisions, R_{AA} (Fig. 3 (middle)) [14], shows a significant suppression for $p_T > 3$ GeV/c in both the 0–10% and 30–50% centrality classes. As the R_{pPb} remains consistent with unity over the entire measured p_T range, it is concluded that the suppression in Pb–Pb collisions occurs due to final-state effects in the medium rather than CNM effects.

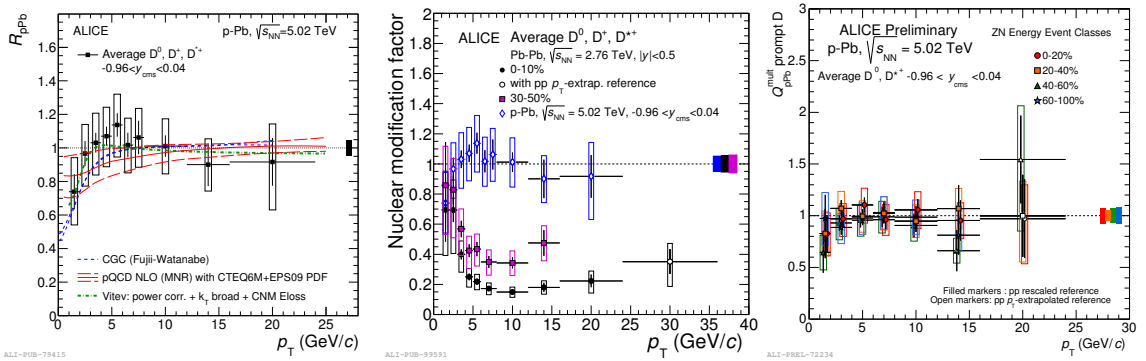


Fig. 3. Average R_{pPb} of D^0 , D^+ and D^{*+} mesons [2] compared with (left) models that include initial-state effects [7, 9, 11–13] and (middle) R_{AA} at $\sqrt{s_{NN}} = 2.76$ TeV [14]. Right: average D-meson Q_{pPb} results in four centrality classes.

Further studies of heavy-flavour production as a function of multiplicity and centrality allow the interplay of hard and soft processes to be examined. One approach is to measure the centrality-dependent nuclear

modification factor, Q_{pPb} . Q_{pPb} is defined as $Q_{pPb}^{\text{mult}} = \frac{dN_{pPb}^D/dp_T}{\langle T_{pPb}^{\text{mult}} \rangle \cdot d\sigma_{pp}^D/dp_T}$. T_{pPb} denotes the nuclear overlap function, which is calculated under the assumption that the charged-particle multiplicity at mid-rapidity scales linearly with the number of participant nucleons [15]. The collision centrality is estimated using the ZNA calorimeter. The average D-meson Q_{pPb} (Fig. 3 (right)) is consistent with unity, and is independent of both centrality and p_T within uncertainties. Finally, we consider the relative D-meson yields as a function of charged-particle multiplicity. The relative yield is defined as the corrected yield per event in a given multiplicity class, divided by the multiplicity-integrated yield per event. Two multiplicity estimators were used: the number of track segments reconstructed in the SPD at mid-rapidity ($|\eta| < 1.0$), and the VOA signal at backward rapidity ($2.8 < \eta < 5.1$). Figure 4 (left) shows the average relative yields obtained for D^0 , D^+

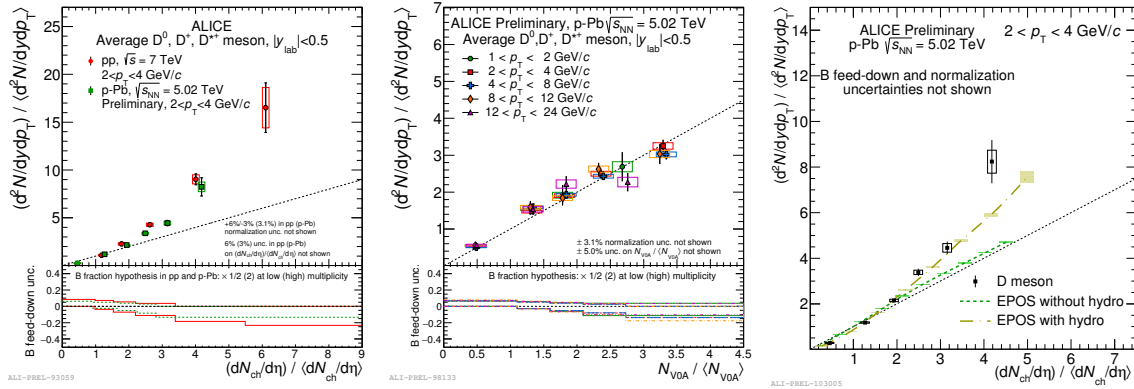


Fig. 4. Relative D-meson yields as a function of multiplicity, estimated with the (left) SPD and (middle) VOA estimator. The pp results in the left-hand plot are taken from [16]. The dashed black lines represent a linear increase ($y = x$), and are displayed to guide the eye. Right: comparison of multiplicity-dependent results from the SPD estimator with EPOS 3 calculations [17, 18], with and without viscous hydrodynamics.

and D^{*+} mesons with the SPD estimator for $2 < p_T < 4$ GeV/c, compared with the equivalent measurement in pp collisions [16]; Fig. 4 (middle) shows the results from the VOA estimator in five p_T bins. For the SPD estimator, the results in both pp and p–Pb collisions exhibit a similar multiplicity dependence, with each showing a faster-than-linear relative D-meson yield increase at high multiplicity. The faster-than-linear increase seen in pp collisions is attributed to multi-parton interactions [16]. The results from the VOA estimator in p–Pb collisions, on the other hand, show a roughly linear increase as a function of multiplicity. The results from the SPD estimator in p–Pb collisions are also compared with EPOS 3 calculations [17, 18] in Fig. 4 (right). It was found that the multiplicity dependence of D-meson production is described better by calculations that include viscous hydrodynamics, especially at higher multiplicity.

References

- [1] ALICE Collaboration, Int. J. Mod. Phys. A29 (2014) 1430044.
- [2] ALICE Collaboration, Phys. Rev. Lett. 113 (23) (2014) 232301.
- [3] ALICE Collaboration, Preprint (2015). [arXiv:1509.07491](https://arxiv.org/abs/1509.07491).
- [4] ALICE Collaboration, Phys. Rev. Lett. 109 (2012) 112301.
- [5] M. Cacciari, M. Greco, P. Nason, JHEP 05 (1998) 007.
- [6] A. M. Sickles, Physics Letters B 731 (2014) 51–56.
- [7] R. Sharma, I. Vitev, B.-W. Zhang, Phys. Rev. C 80 (2009) 054902.
- [8] Z.-B. Kang, et al., Phys. Lett. B 740 (2015) 23–29.
- [9] K. J. Eskola, H. Paukkunen, C. A. Salgado, JHEP 04 (2009) 065.
- [10] I. Vitev, Phys. Rev. C 75 (2007) 064906.
- [11] M. L. Mangano, P. Nason, G. Ridolfi, Nucl. Phys. B373 (1992) 295–345.
- [12] D. Stump, et al., JHEP 10 (2003) 046.
- [13] H. Fujii, K. Watanabe, Nucl. Phys. A920 (2013) 78–93.
- [14] ALICE Collaboration, Preprint (2015). [arXiv:1509.06888](https://arxiv.org/abs/1509.06888).
- [15] ALICE Collaboration, Phys. Rev. C91 (6) (2015) 064905.

- [16] ALICE Collaboration, JHEP 09 (2015) 148.
- [17] H. Drescher, et al., Phys. Rept. 350 (2001) 93–289.
- [18] K. Werner, et al., Phys. Rev. C89 (2014) 064903.